Effects of Urban Vegetation on Mitigating Exposure of Vulnerable Populations to Excessive Heat in Cleveland, Ohio

JUAN DECLET-BARRETO

Natural Resources Defense Council, Washington, D. C.

KIM KNOWLTON

Natural Resources Defense Council, and Department of Environmental Health Sciences, Mailman School of Public Health, Columbia University, New York, New York

G. DARREL JENERETTE

Department of Botany and Plant Sciences, University of California, Riverside, Riverside, California

ALEXANDER BUYANTUEV

Department of Geography and Planning, University at Albany, State University of New York, Albany, New York

(Manuscript received 25 March 2015, in final form 6 June 2016)

ABSTRACT

Hot weather is a threat to human health, especially in cities, where urban heat islands (UHIs) are elevating temperatures already on the rise from global climate change. Increased vegetation can help reduce temperatures and exposure to heat hazards. Here, an ensemble of geographically weighted regressions (GWR) on land surface temperature (LST) is conducted for May–October to estimate potential LST reductions from increased vegetation and to assess the effect of temperature reductions among vulnerable populations in Cleveland, Ohio. Possible tree canopy increases are applied to the results, and it is found that LST reductions can range from 6.4° to 0.5°C for May–October and are strongest from May to July. Potential LST reductions vary spatially according to possible canopy increases and are highest in suburban fringe neighborhoods and lower in downtown areas. Among populations at high heat-related health risks, the percentage of the population 65 years of age or older in Cleveland is negatively associated with LST, while percentages of Hispanics and those with low educational achievement are most positively associated with higher LST. The areas that have a high percentage of Hispanic also have the lowest potential temperature reductions from increased vegetation. Neighborhoods with the highest potential temperature reductions had the highest percentages of whites. Three subpopulations associated with high heat health risks are negatively correlated (African Americans and the elderly) or not correlated (persons living in poverty) with LST, and the relationships to LST reduction potential for all three are not statistically significant. Estimates of the effect of vegetation increases on LST can be used to target specific neighborhoods for UHI mitigation under possible and achievable policy-prescribed tree canopy scenarios in Cleveland.

1. Introduction

Exposure to high summertime temperatures is a significant threat to human health, especially in cities, where urban heat islands (UHIs) are elevating temperatures already on the rise from global climate change. Heat-retaining, impervious land covers like paved roadways and unvegetated surfaces and alterations to wind and energetic flows from vertical surfaces of buildings elevate local temperatures in UHIs. These anthropogenic,

Denotes Open Access content.

Supplemental information related to this paper is available at the Journals Online website: http://dx.doi.org/10.1175/WCAS-D-15-0026.s1.

Corresponding author address: Juan Declet-Barreto, Natural Resources Defense Council, 1152 15th St. NW Suite 300, Washington, DC 20005.
E-mail: jdeclet-barreto@nrdc.org

DOI: 10.1175/WCAS-D-15-0026.1

regional-scale transformations to natural land covers are known to be responsible for the UHI microclimatic signature of cities (Oke 1997; Arnfield 2003; Li and Bou-Zeid 2013). Although the classic UHI signature is an observable temperature gradient between the urban built environment and surrounding rural areas (Balling and Brazel 1987), UHI magnitudes within cities show significant spatial heterogeneity and are driven by land use/land cover and density of the built environment (Ruddell et al. 2010).

The sensitivity of populations to extreme heat-related illness (e.g., morbidity) and death (e.g., mortality) is influenced by socioeconomic characteristics (e.g., ethnicity, poverty, linguistic isolation, and old age), air conditioner use, preexisting medical conditions, the presence or absence of heat-mitigating vegetation, and age-based or other forms of social isolation (Reid et al. 2012; Harlan et al. 2006, 2013; White-Newsome et al. 2014b,a). Thus mitigating high temperatures from UHIs is a desirable public health goal. Mitigating high temperatures can also address environmental justice/equity issues because of the prevalence of race- and class-based disparities in adverse heat health outcomes. For example, across the United States, Hispanic, African American, and Asian populations often live in neighborhoods with high percentages of impervious surfaces and no tree canopy, two land covers associated with higher heat risks (Jesdale et al. 2013). Adverse heat health outcomes, such as mortality (e.g., Johnson and Wilson 2009; Kaiser et al. 2007; Harlan et al. 2013; Hondula et al. 2012; Yip et al. 2008) and morbidity (e.g., Hattis et al. 2012; Johnson and Wilson 2009), are found to be higher among minority and impoverished communities.

Although the degree to which UHIs affect heat health outcomes is not well known (Stone et al. 2014), modeling suggests that vegetation-based interventions to reduce urban temperatures can potentially reduce heat-related mortality and morbidity (Boumans et al. 2014; Stone et al. 2014). Reducing UHI magnitudes can also reduce demand for air conditioner use, which provides the added benefit of reducing heat waste that feeds back as anthropogenic heat into the UHI. In addition, reduced air conditioner use can lower demand for electricity, which can lead to lower emissions of carbon dioxide and other greenhouse gases and copollutants (Salamanca et al. 2014). Lower urban temperatures can also reduce ozone formation from photochemical interactions of volatile organic compounds and other ozone precursors in the lower atmosphere of cities (Oke 1997), which, in some cases, is known to exacerbate heat-related mortality (Filleul et al. 2006; Pattenden et al. 2010). The potential public health and emissions reductions benefits of mitigating extreme heat and UHIs is motivating the development of increased climate resilience in many cities across North America: many cities in the United States are responding to increases in the number of extreme heat days by adopting heat-mitigation plans as part of climate resilience and adaptation planning (Hewitt et al. 2014).

UHI mitigation typically consists of reducing the amount of solar radiation that is absorbed by impervious surfaces. Two common mechanisms for achieving this include altering surface covers by increasing the fraction of total solar radiation reflected (i.e., albedo) and increasing vegetative cover. Increasing albedo can reduce the amount of heat absorbed during daytime hours, thereby reducing emitted nighttime radiation from impervious materials. Albedo can be increased through the application of highly reflective vertical and horizontal materials. Increasing vegetation can provide shading and transpirational cooling, two ecosystem services that can reduce heat loads in cities. Canopied vegetation, however, has different day and nighttime effects. Buyantuyev and Wu (2010) suggest that, since vegetation is cooler during the day, this effect may continue into the night and result in lower temperatures. However, at night, heat can be trapped under the vegetation canopy and radiated back into the environment, increasing nighttime warming. Although there is uncertainty regarding day versus night effects, vegetated spaces in cities have been shown to create localized park cool islands (PCI), countering the effect of the UHI (Chow et al. 2011; Declet-Barreto et al. 2013). Microclimate simulations have shown that, under certain synoptic climate conditions, PCIs can have localized ''spillover'' advective cooling effects that extend beyond vegetated land covers (Declet-Barreto et al. 2013).

Vegetation provides two principal ecosystem services that affect surface and near-surface temperatures. Tree canopies absorb and reflect solar radiation, effectively *shading* surfaces from direct radiant energy contact. *Transpirational cooling* works as liquid water evaporates to a gas in the cells of leaves (Declet-Barreto et al. 2013). Remote-sensing-based approaches to UHI mitigation have shown that the extent and magnitude of these ecosystem services are dependent on local climate, land use/land cover, water, and the extent and composition of vegetation (Jenerette et al. 2007; Imhoff et al. 2010; Voogt and Oke 2003).

Estimating land surface temperature (LST) from remote-sensing platforms allows researchers to assess intraurban variability in surface UHI intensities, a spatial scale improvement over the often sparse and irregular distribution of weather station networks in many metropolitan areas. The increased spatial detail comes with a loss in the temporal resolution of temperature

data, as estimates are limited to the time that a space or airborne sensor flies over the study area. In spite of these limitations, LST has been shown to correlate to heat vulnerability at the neighborhood scale (Johnson et al. 2009; Buscail et al. 2012; Hondula et al. 2012; Harlan et al. 2013), modulate lower-atmosphere urban temperatures, and be a primary factor in determining human comfort in cities (Voogt and Oke 1998). Furthermore, LST has important heat and public health applications, as it can be useful for assessing the characteristics of temporally stable built environments that can shape human exposure to heat and also for targeting heat-health interventions (White-Newsome et al. 2013).

The relationship between LST and vegetation is well established: vegetation is a known regulator of temperatures. The normalized difference vegetation index (NDVI)—an indicator of photosynthetically active vegetation (Tucker 1979)—is a common measurement of vegetation derived from remotely sensed data. Ma et al. (2008) and Sun and Kafatos (2007) have reported temporally dependent linear relationships between LST and NDVI at the urban and continental scales and that these relationships are inverse and stronger in the summer than in winter. In Phoenix, Arizona, vegetation cover has been found to contribute to a maximum reduction of 25°C over bare soil in summertime Landsat-derived summertime LST (Jenerette et al. 2011), and, among social and built-environment characteristics, the largest influence on LST reductions was a soil-adjusted vegetation index similar to NDVI (Jenerette et al. 2007). In Shanghai, China, a regression conducted by Yue et al. (2007) found potential LST reductions of up to 12°C from fully vegetated landscapes as measured by NDVI derived from the Landsat ETM+. A study in cities in temperate broadleaf and mixed forest biomes—including coastal cities like Baltimore (Maryland), Boston (Massachusetts), Milwaukee (Wisconsin), New York (New York), and Cleveland (Ohio)—consistently found inverse relationships between NDVI and LST across urban, suburban, and rural land covers (Imhoff et al. 2010). Onishi et al. (2010) simulated LST reductions from planting grass and trees (based on NDVI) in parking lots in Nagoya, Japan, finding slight overall LST reductions. These studies provide evidence that vegetation can regulate LST.

In this paper, we evaluate the role of increased canopied vegetation distributions in reducing high summertime temperatures in neighborhoods in urban areas of Cleveland, Ohio. We use remotely sensed data to quantify the relationship between daytime land surface temperature and vegetation. We conduct an ensemble of geographically weighted regressions (GWR) on land surface temperature and vegetation to estimate the effect of vegetation on surface temperatures across the city. Based on existing and possible canopy increases from a tree canopy assessment conducted by Cuyahoga County's planning agency, we estimate surface temperature reduction potential in Cleveland neighborhoods. Finally, we evaluate our potential LST reductions against socioeconomic and demographic variables associated with heat health risks to identify potential LST reductions among at-risk vulnerable populations.

2. Study area

Cleveland is a city of 390 113 [population density 13 227.1 persons km^{-2} (U.S. Census Bureau 2014)] located in northeastern Ohio in the U.S. Midwest (Fig. 1). The city lies along the southern shore of Lake Erie, is the second most populated city in the state, and serves as the county seat for Cuyahoga County. Cleveland's climate is characterized as humid continental [Köppen Dfa (Kottek et al. 2006)]. Urban tree canopy in Cleveland represents 19% of the city's total area, well below the average for Cuyahoga County (37.6%; Cuyahoga County Planning Commission 2013a). In comparison to other Midwestern cities, Cleveland has the least amount of parkland area per resident at 27.9 m^2, versus Columbus, Ohio (59.1 m^2), Cincinnati, Ohio (58.7 m^2), Milwaukee, Wisconsin (66.0 m^2), and Pittsburgh, Pennsylvania (35.6 m^2; Cleveland City Planning Commission 2014b). During days matching acquisition dates of Landsat scenes used in our analysis, minimum and maximum temperatures were −1.0°C (8 March 2010) and 33.3°C (3 September 2011), respectively (see supplemental material 1) (NCEI 2015). Sheridan et al. (2009) estimate that, annually, Cleveland experiences, on average, 11.1 days with ''oppressive'' air masses associated with heat-related mortality. Bobb et al. (2014) estimate that a projected upward shift of 2.8°C in summertime daily temperatures in Cleveland could result in 43.6 excess deaths per year.

Longitudinal heat mortality studies have found that in many cities around the globe—including Cleveland—heat-related mortality has decreased over time, an adaptation that is thought to be explained in part by increased prevalence of air conditioners (Bobb et al. 2014; Gasparrini et al. 2015). Indeed, in Cleveland, Gasparrini et al. (2015) estimated a drop in relative risk of heat-related mortality from approximately 1.4 in 1993 to approximately 1.1 in 2006. Notwithstanding observed decreases, heat-related health impacts in Cleveland and other locations persist, and uncertainty about how these will evolve under a changing climate remains. Therefore, improving strategies for reducing heat-related health risks and decreasing preventable mortality and morbidity from extreme weather is a desirable public health goal.

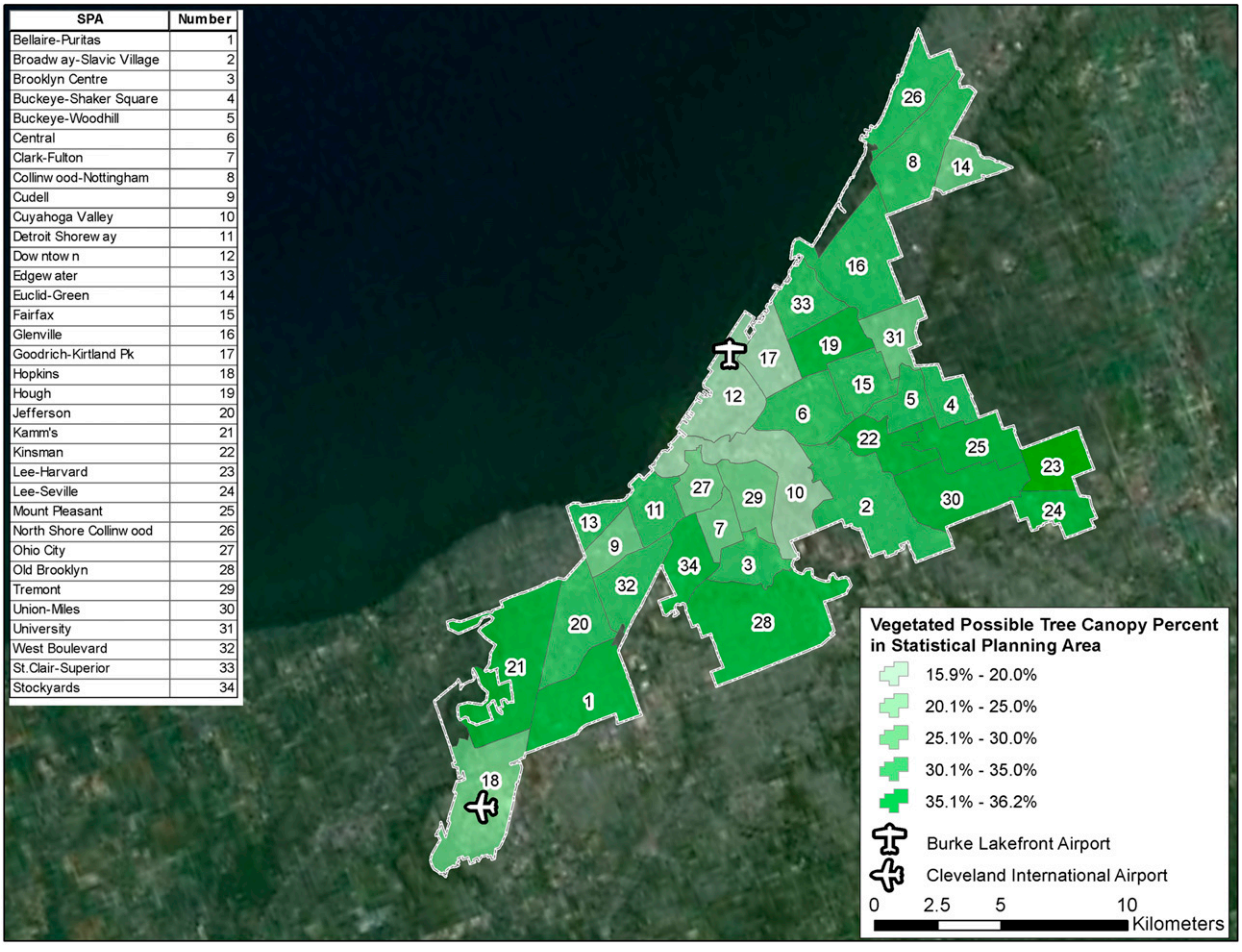

FIG. 1. VPTC in SPAs in the Cleveland, Ohio, study area. The Cleveland International and Cleveland Burke Lakefront Airports are indicated on the map.

Cleveland has a long history of racial segregation demarcated informally by the Cuyahoga River and today remains one of the most segregated cities in the United States (Frey and Myers 2005). Like many other American cities during the postwar period, Cleveland experienced high rates of ''white flight'' (the self-removal of white residents from nonwhite populations), contributing to segregation of African American and white populations (Galster 1990). In 2010, African American residents made up the majority of the city's population (53.3%), followed by non-Hispanic white (33.4%), Hispanic (10.0%), and Asian populations (1.8%, U.S. Census Bureau 2014). Twelve percent of the Cleveland population is 65 years of age or older (U.S. Census Bureau 2014). A large fraction of the population is under poverty, at 34.2% (Minnesota Population Center 2016a,b), and the presence of mechanical cooling [i.e., air conditioners (AC)] in residential parcels is not prevalent [on average, only 12.9% of all residential parcels have either central or ''through-wall'' AC units (Cuyahoga County Planning Commission 2013a)]. Spatial distributions of selected race/ethnicity and socioeconomic status variables are mapped in Fig. 2. Figures 2a–c highlight the segregated racial structure of the city; Figs. 2b–g show distributions of variables associated with higher heat-related risks in statistical planning areas (SPAs).

3. Methods and data

a. Data on land surface temperature and vegetation

Urban climatology has identified different types of UHIs according to the component of the urban environment under study: that is, urban canopy layer, urban boundary layer, surface, and subsurface, (Oke 2006; see review in Heisler and Brazel 2010). In this paper, we focus on the daytime Cleveland UHI as measured at the urban surface. Temperatures at the urban surface, also known as ''skin'' temperatures,

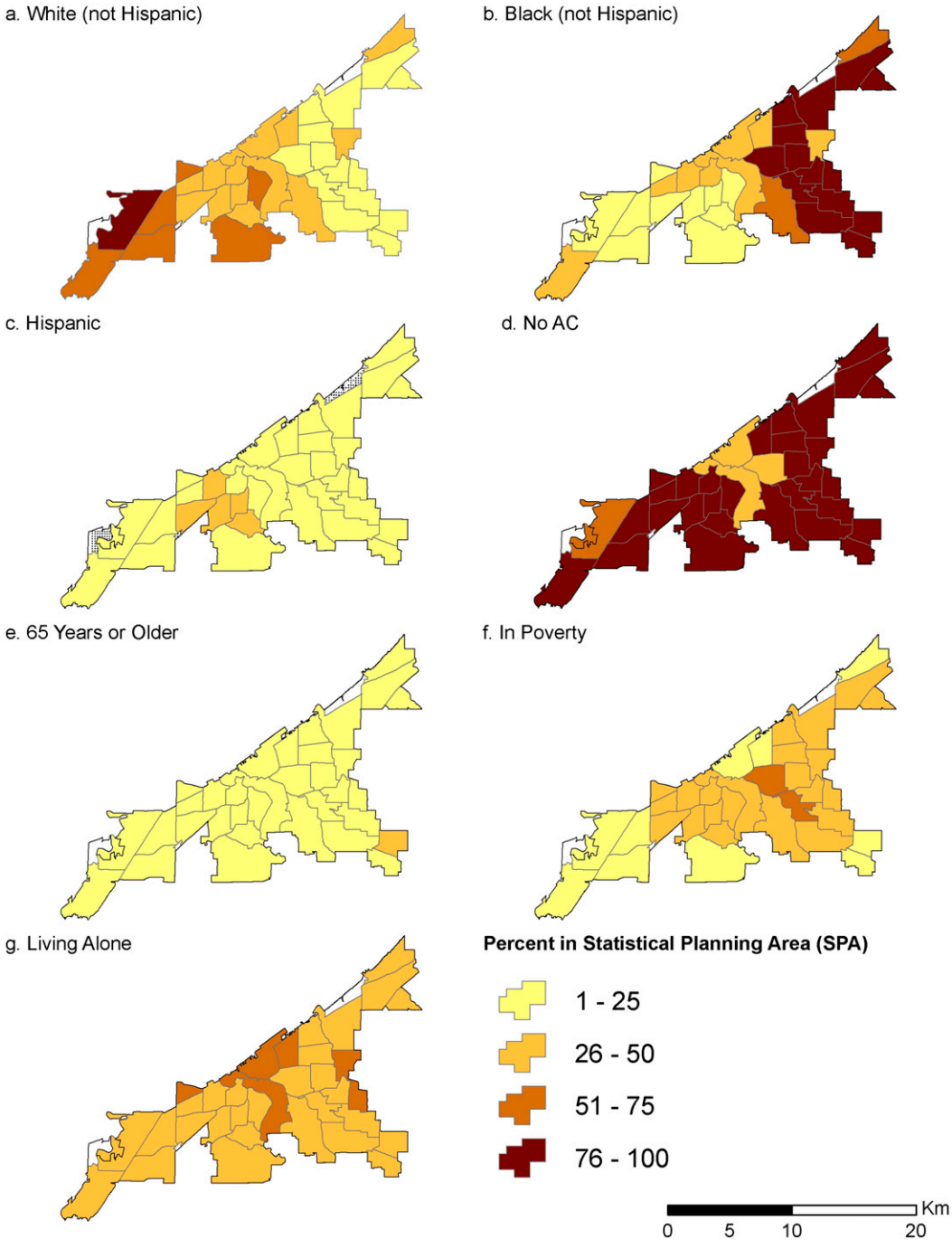

FIG. 2. Race/ethnicity and socioeconomic variables in statistical planning areas in Cleveland associated with disparities in extreme heat vulnerability.

represent upper surface temperatures of urban land covers like buildings, streets, and lawns (Heisler and Brazel 2010) and are typically measured through handheld, air- or spaceborne remote sensors (Gallo et al. 1993). In this study, we use high-resolution, spatially contiguous data from the Landsat satellite imagery program to characterize the relationship between LST and NDVI.

Skin temperatures estimated from satellite data are subject to larger day-to-day variability than NDVI-based vegetation estimates, and heterogeneity in urban land covers introduces large spatial variability in the LST–NDVI

relationship. To address this, we generated an ensemble of 12 daytime Landsat Thematic Mapper (TM) scenes from May through November of 2009–11 and calculated LST and NDVI for each Landsat scene. Level 1T images acquired by the TM instrument onboard the Landsat 5 satellite were obtained from USGS (2016) and used to estimate LST and NDVI. The TM sensor records radiance information in the visible through shortwave infrared portions of the electromagnetic spectrum in six spectral bands (0.45–2.35 μm) at 30 m pixel^{-1} nominal ground resolution. Emitted energy in the midinfrared wavelengths (10.4–12.5 μm) is acquired at 120 m pixel^{-1}, but for convenience this spectral band is resampled and delivered by USGS at 30 m pixel^{-1} resolution. We processed 12 images (Path/Row: 19/31) with no or minimal cloud cover spanning the spring, summer, and fall seasons (25 June 2009, 27 July 2009, 13 September 2009, 8 March 2010, 27 March 2010, 31 August 2010, 3 November 2010, 19 November 2010, 1 July 2011, 3 September 2011, 5 October 2011, and 6 November 2011). Occasional clouds with shadows were manually masked out. The atmospheric component of reflected and emitted energy in each image was modeled and removed using the MODTRAN-based atmospheric correction in ERDAS Imagine 2014 image processing software. LST was calculated from the atmospherically corrected midinfrared band 6 of the image as a numerical solution to the Planck temperature–emissivity equation with assumed constant emissivity ε of 0.98. NDVI was calculated using two atmospherically corrected TM bands as follows:

$$\mathrm{NDVI} = (\mathrm{NIR} - \mathrm{Red})/(\mathrm{NIR} + \mathrm{Red}), \qquad (1)$$

where near-infrared (NIR) is TM band 4 (0.76–0.90 μm), and Red is TM band 3 (0.63–0.69 μm) of Landsat. The index range is ± 1.0, and we recoded negative values to zero (less than one percent for all but one Landsat scene) in order to avoid negative values in regression analyses.

The city boundary GIS file (Cuyahoga County Geographical Information Systems 2016) was used to extract pixels within our study area. Because of the large number of pixels in each scene (224 839) and to account for spatial variability in the LST–NDVI relationship, we conducted 1000 correlation iterations for each scene using randomly sampled pixels (n = 5000), after Jenerette et al. (2011). Figure 3 shows LST–NDVI correlation coefficients. Each data point represents the mean coefficient for the group of 1000 iterations conducted for each Landsat scene (average standard error of the mean for each group of 1000 iterations was 4.5×10^{-4}). As in previous studies (e.g., Jenerette et al. 2011; Boumans et al. 2014), the LST–NDVI relationship is strongest in the summer months and weakest in the winter. Based on Fig. 3, we selected Landsat scenes from May through October—excluding the 27 July scene because of the low r^2—for a geographic regression analysis, described in the next section. Because of the presence of surface water from the Cuyahoga River and other streams in Cleveland, we identified surface water using the USGS National Land Cover Database 2011 (Jin et al. 2013) and eliminated overlapping Landsat observations from the analysis.

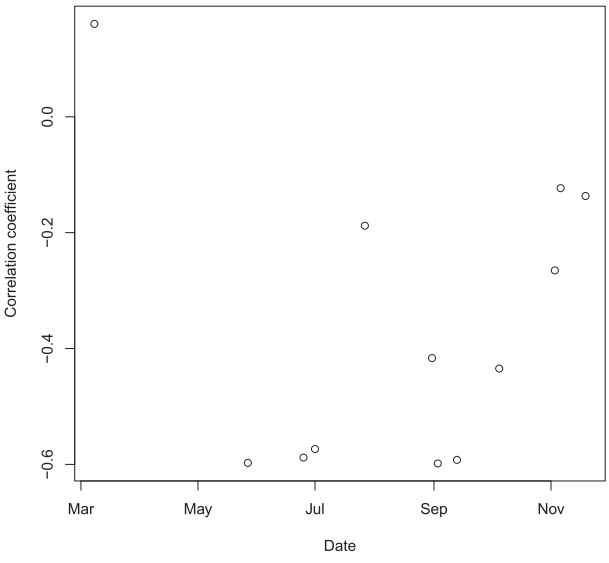

FIG. 3. Bivariate correlations for the LST–NDVI relationship in an ensemble of Landsat scenes from May to November. The association between LST and vegetation is weakest in the winter and strongest in the summer.

b. *Data on heat-sensitive populations and neighborhoods*

We extracted variables in census block groups (CBGs) from the 2010 U.S. Census and American Community Survey 2006–10 5-yr estimates (Minnesota Population Center 2010a,b) identified in the heat health literature as individual risk factors associated with heat death or illness. We aggregate these variables at the statistical planning area (SPA) level in order to explore neighborhood-scale sensitivity to heat risks. There are 34 SPAs, created by the Cleveland City Planning Commission and equivalent to neighborhoods (Cleveland City Planning Commission 2014a; see Fig. 1). CBG boundaries often overlap SPA boundaries, so we apportioned CBG variables to SPAs using a simple spatial weighting scheme based on the fraction of the SPA that a CBG completely or partially within an SPA occupies. In addition, we used Cuyahoga County parcel data (Cuyahoga County Planning Commission 2013a) to construct an indicator representing the percent of

residential parcels with no central or wall-through AC units in Cleveland. As an exploratory step, we report on Spearman's bivariate correlations between heat-risk factors and mean LST.

c. Data on existing and possible tree canopy

We obtained tree canopy data for parcels in Cleveland from the Cuyahoga County Planning Commission's "Urban Tree Canopy Assessment" (UTCA; Cuyahoga County Planning Commission 2013b). The UTCA data provide geospatially referenced files of parcels and contain variables representing percentages of existing tree canopy (ETC) and vegetated possible tree canopy (VPTC). The VPTC variable represents the fraction of a parcel that already contains grass or shrubs, where tree planting is more likely to occur as a result of the lower cost of planting and the abundance of vacant vegetated land (D. Meaney 2015, personal communication). We used these data in two ways: we first express NDVI in terms of ETC and then estimate potential LST reductions based on plausible tree canopy increase scenarios in the VPTC variable.

d. Geographically weighted regression analysis

We conduct geographically weighted regression (Fotheringham et al. 2003) on all pixels in Landsat scenes from May to October (with the exception of the 27 July scene) identified in the LST–NDVI correlations in Fig. 3 to estimate the effect of vegetation on LST. GWR is a technique that computes a local regression equation for each observation in a dataset, where the influence of each neighboring observation is weighted according to a user-defined matrix defining spatial proximity to the regression point. GWR is a modification of the ordinary least squares (OLS) regression specified as follows:

$$y_i = \beta_0(u_i, v_i) + \beta_1(u_i, v_i)x_{i1} + \ \ldots \ + \beta_n x_{in} + \varepsilon_i, \qquad (2)$$

where y_i is the value of the dependent variable at location i; β_0, β_1, and β_n are local regression coefficients; (u_i, v_i) is a specification of the location of regression point i; and ε_i is an error term.

GWR is well suited to characterize spatially heterogeneous phenomena like LST–NDVI relationships, where OLS or multiple linear regression may not adequately describe the variability of the relationship across space (Foody 2003; Maselli 2002). Estimating UHI intensities using global models can underestimate the influence of explanatory variables, and significant improvements in model fits from GWR versus global models have been reported (Su et al. 2012; Szymanowski and Kryza 2011; Ivajnšič et al. 2014; Li et al. 2010). GWR has been used to estimate the effects of land use/land cover on urban temperatures, finding that vegetation and impervious surfaces are the strongest factors regulating temperatures (Buyantuyev and Wu 2010; Yuan and Roy 2007; Mohamed 2013).

Following Eq. (2), we regress LST on NDVI as follows:

$$\mathrm{LST}_i = \beta_0(u_i, v_i) + \beta_1(u_i, v_i)\mathrm{NDVI}_i + \varepsilon_i, \qquad (3)$$

where LST_i is the dependent variable, β_0 is the intercept, and β_1 is the local regression coefficient for independent variable NDVI_i.

GWR requires the specification of a spatial weights matrix that defines which observations are considered neighbors of an observation for which local regression coefficients are desired. Neighboring observations in regularly spaced grids are best represented using a fixed-bandwidth spatial kernel (Fotheringham et al. 2003). Landsat data in our study were provided in a raster grid with a 30-m spatial resolution. Using GIS software, we converted all rasters to points representing the centroid of each pixel in an evenly spaced (30 m × 30 m) grid. To assess model sensitivity to bandwidth distance, we conducted multiple GWR runs with distance bandwidths of 100, 250, 500, 1000, 1250, and 1500 m. As distance increases, r^2 values decrease, converging toward 0.7 for distances ≥500 m (supplemental material 2). Based on this sensitivity analysis, we considered pixels within a fixed distance of 500 m to be influential in determining the LST–NDVI relationship and thus conducted all GWR runs using a 500-m-distance bandwidth. We then used the GWR results to map bare surface temperature [BST; i.e., the surface temperature of bare soil, or where NDVI = 0 (Jenerette et al. 2011)] and local NDVI regression coefficients. We estimated potential LST reductions by narrowing the theoretical range of NDVI (±1.0) to more realistic values based on "Urban Tree Canopy Assessment" data, which we describe next.

e. Estimation of cooling potential

We combined the GWR results and the tree canopy assessment data to estimate and map potential LST reductions. The tree canopy data provide potential canopy cover percentages that can be used to narrow the theoretical range of NDVI (±1.0) to more realistic values, but require the expression of NDVI as a function of canopy percentages. Mean NDVI values in parcels for the May–October Landsat scenes showed linear correlations with existing tree canopy (r^2 0.59–0.64; supplemental material 3). To express NDVI values in terms of percent tree cover, we conducted, for each May–October Landsat scene, a linear regression of mean NDVI in parcels on the ETC variable (mean coefficient = 0.894).

We then used the NDVI–ETC regression coefficient for each Landsat scene to estimate cooling potential based on VPTC values for each parcel. This allowed us to estimate cooling from potential planting of tree canopy values that are more feasible than the theoretical ±1.0 range of NDVI values. We then summarized cooling potential results to SPAs in order to estimate LST reductions in Cleveland's statistical planning areas. In the last part of the analysis, we report bivariate correlation coefficients between sociodemographic and LST–NDVI GWR coefficients in SPAs to understand how potential vegetation-induced LST reductions vary among different heat-vulnerable subpopulations in Cleveland.

4. Results

LST varies among heat-vulnerable subpopulations and heat risk factors (Table 1). Among the heat-vulnerable populations considered, Hispanic populations and populations with low educational achievement are the most strongly associated with elevated temperatures. Statistically significant LST correlations with the variable ''Percent Hispanic'' ranged from 0.44 to 0.60 for August–October, and ''Percent no high school diploma'' versus all Landsat scenes ranged from 0.34 to 0.67 (all were statistically significant). ''Percent African American'' shows small negative, but mostly nonstatistically significant, correlations with LST. ''Percent elderly'' has negatively strong and significant correlations with surface temperatures (−0.40 to −0.73), ''percent living alone'' shows only one significant correlation with LST, and the combination of ''Percent elderly'' and ''alone'' is negatively strongly correlated, ranging from −0.42 to −0.67 for all but one of the May–October Landsat scenes. Both ''percent no AC'' and ''percent white'' exhibited nonsignificant correlations.

GWR model diagnostics show improved performance over OLS: r^2 values for OLS regressions ranged from 0.19 to 0.36, while GWR explained 0.65–0.75 of variability in LST reductions from NDVI (Table 2). Changes in the Akaike information criterion (AICc) from higher values (OLS) to lower (GWR) indicate improved fit of observations in the geographically explicit model. The ensemble of GWR runs produced an intercept (β_0, interpreted as BST) and a regression coefficient (β_1) for NDVI for each regression point in each Landsat scene. Spatial distributions of BST estimates are presented in Fig. 4. Following Mennis's (2006) suggestions for mapping GWR results, we estimated statistical significance by dividing each local regression coefficient by its standard error and comparing it with the t tablevalue associated with the 95% confidence interval. For the May–October period, BST ranged from 17.0° to 58.0°C; the lowest mean was 23.8°C (5 October), and the highest was 47.2°C (1 July). For most scenes, BST appears lower along the Lake Erie coastline, shown more clearly in the 31 August and 3 September results (Figs. 4d,e). Local regression coefficients (β_1) from GWR for NDVI are shown in Fig. 5. Daily variations in each scene were driven by NDVI values: in any given scene, LST increases (reductions) corresponded to low (high) NDVI values. Across scenes, LST varied according to season, as higher incoming solar radiation was detected by the Landsat sensor during the summer scenes but attenuated during the fall/winter months.

For all Landsat scenes, the cooling effect of vegetation on LST reductions ranges between 26.1° and 0.0°C for maximum possible vegetation (i.e., NDVI = 1.0; negative signs imply LST reductions), and are estimates based solely on GWR results. In a few areas, the GWR models predict increases in LST of up to 6.0°C, but these accounted for only up to 2.1% of observations and were restricted to an industrial and mostly bare soil small area near the Lake Erie and Cuyahoga River shores.

Combining the NDVI local coefficients with vegetated possible tree canopy data in SPAs constrains potential LST reductions estimated from the GWR results alone shown in Fig. 5. For May–October, vegetated possible tree canopy percentages suggest potential LST reductions ranging from 6.4° to 0.5°C (Fig. 6). The cooling effect is both stronger and more spatially variable from May through July and diminished from August to October. Visually, potential LST reductions appear lowest around the downtown area (and also in some surrounding SPAs) and highest in outer fringe SPAs, a pattern consistent with the spatial distribution of VPTC (Fig. 1). For May–October, the neighborhoods of Edgewater, Euclid-Green, and Kamm's received the largest LST reductions, while Buckeye-Shaker Square, Clark-Fulton, Goodrich-Kirtland Park, and Downtown received the lowest LST reduction estimates (Table 3; see supplemental material 4 for a summary of VPTC and VPTC-constrained NDVI values in SPAs).

The effect of vegetation on regulating LST varied among heat-vulnerable subpopulations and heat risk factors. We now present socioeconomic variables related to heat risks for select neighborhoods with the highest and lowest potential LST reduction estimates. We focus on these neighborhoods because, as shown on Table 3 for the May–October period, they consistently receive the lowest or highest values in LST reduction potentials. Among the three neighborhoods with highest cooling potential, there are clear racial differences: while Euclid-Green in the eastern fringe of the city is 92% black, Edgewater and Kamm's, on the western end, are 65% and 79% white (Table 4). In the neighborhoods with

TABLE 1. Spearman's correlations for socioeconomic variables related to heat risks and May–October land surface temperature in SPAs in Cleveland, Ohio. Here, "black" indicates black (not Hispanic), and "white" indicates white (not Hispanic).

	Percent black	Percent white	Percent Hispanic	Percent in poverty	Percent no AC	Percent no HS diploma	Percent elderly	Percent alone
Percent black								
Percent white	−0.91[a]							
Percent Hispanic	−0.87[a]	0.75[a]						
Percent in poverty	0.18	−0.26	0.00					
Percent no AC	0.12	−0.35[b]	−0.02	0.22				
Percent no HS diploma	−0.13	−0.08	0.37[b]	0.67[a]	0.33			
Percent elderly	0.41[b]	−0.27	−0.60[a]	−0.19	−0.04	−0.48[a]		
Percent alone	0.05	0.10	−0.17	0.04	−0.30	−0.21	−0.11	
Percent elderly and alone	0.41[b]	−0.29	−0.60[a]	0.02	−0.09	−0.41[b]	0.92[a]	0.03
Mean LST (27 May)	−0.18	0.07	0.36[b]	0.05	0.00	0.44[b]	−0.49[a]	−0.17
Mean LST (25 Jun)	−0.04	−0.11	0.20	0.14	0.15	0.40[b]	−0.52[a]	−0.15
Mean LST (1 Jul)	−0.01	−0.09	0.18	0.10	0.08	0.34[b]	−0.40[b]	−0.16
Mean LST (31 Aug)	−0.26	0.10	0.44[a]	0.31	0.07	0.67[a]	−0.61[a]	−0.04
Mean LST (3 Sep)	−0.33	0.21	0.55[a]	0.14	−0.07	0.48[a]	−0.73[a]	0.04
Mean LST (13 Sep)	−0.28	0.20	0.47[a]	−0.03	−0.02	0.35[b]	−0.60[a]	−0.17
Mean LST (5 Oct)	−0.46[a]	0.30	0.60[a]	−0.09	0.04	0.37[b]	−0.40[b]	−0.40[b]

	Percent elderly and alone	Mean LST (27 May)	Mean LST (25 Jun)	Mean LST (1 Jul)	Mean LST (31 Aug)	Mean LST (3 Sep)	Mean LST (13 Sep)
Per elderly and alone							
Mean LST (27 May)	−0.46[a]						
Mean LST (25 Jun)	−0.46[a]	0.86[a]					
Mean LST (1 Jul)	−0.30	0.92[a]	0.89[a]				
Mean LST (31 Aug)	−0.53[a]	0.89[a]	0.74[a]	0.78[a]			
Mean LST (3 Sep)	−0.67[a]	0.87[a]	0.77[a]	0.74[a]	0.86[a]		
Mean LST (13 Sep)	−0.57[a]	0.94[a]	0.84[a]	0.87[a]	0.79[a]	0.89[a]	
Mean LST (5 Oct)	−0.42[b]	0.86[a]	0.67[a]	0.74[a]	0.76[a]	0.74[a]	0.84[a]

[a] $p \leq 0.01$.
[b] $p \leq 0.05$.

the lowest LST reduction potential, Buckeye-Shaker Square is overwhelmingly black at 80%, Goodrich-Kirtland Park has high rates of social isolation (67% are one-person households), and Downtown has a fairly even split between blacks and whites (44% and 43%, respectively). Clark-Fulton, another neighborhood with some of the lowest LST reduction potentials, registers high rates of Hispanics (48.3%), poverty (nearly 40%), and low educational achievement (38.2%).

5. Discussion and conclusions

Similar to other studies exploring local variation on urban temperature–vegetation dynamics, in our study we find significant model performance improvements from local (GWR) over global (OLS) models (Su et al. 2012; Szymanowski and Kryza 2011; Ivajnšič et al. 2014; Li et al. 2010). Estimations from our geographically explicit model runs demonstrate local variation in the relationship between surface temperature and vegetation and show that the potential for vegetation-induced reductions in skin temperatures is highly heterogeneous, both spatially and temporally. The ensemble of Landsat imagery from May to November allowed us to establish variability in the seasonality of the LST–NDVI relationship: vegetation is an effective regulator of temperatures during the summer, but the effectiveness attenuates in the winter months. The effect of vegetation-based temperature regulation, however, can be overestimated by the use of spectral indices like NDVI if vegetation densities are not constrained to represent realistic tree canopy densities. We addressed this by expressing NDVI values in terms of existing tree canopy percentages and then deriving NDVI values based on vegetated possible tree canopy estimates, which were applied to the GWR parameter estimates to estimate cooling potential. The spatial variability of our cooling potential results reflects the variability of the tree canopy estimates, indicating that the highest temperature reduction potential is in neighborhoods with abundant natural land covers (but not currently covered with tree canopies). Conversely, the lowest potential for cooling was in areas dominated by impervious land covers, such as paved surfaces, parking lots, buildings, and rights-of-way. The comparison of the

TABLE 2. Goodness-of-fit statistics for OLS and GWR runs of Landsat scenes.

	OLS		GWR		
Date	r^2	AICc	r^2	AICc	Effective number
27 May	0.35	1 117 336	0.75	890 830	1007.39
25 Jun	0.35	1 086 874	0.73	872 844	1008.99
1 Jul	0.33	1 212 127	0.74	982 141	1012.10
31 Aug	0.32	943 450	0.74	709 909	1012.56
3 Sep	0.36	868 763	0.72	668 051	1012.49
13 Sep	0.35	866 554	0.69	692 026	1010.42
5 Oct	0.19	884 622	0.65	683 439	1014.41

cooling potential estimates with heat risk factors suggest that extreme heat exposure in Cleveland varies across different socio-demographic groups and is particularly differentiated among racial and ethnic minorities and other heat-vulnerable groups. Some of the heat risk factors we considered, including percent African American, percent 65 years or older, social isolation, lack of AC, and poverty did not show strong relationships with higher heat exposure across the city, but Hispanics and those with low educational achievement appear to have high exposure to high temperatures, and their neighborhoods are unlikely to receive temperature reductions because of low vegetation potentials. Although we did not subject heat risk factors and GWR results to a formal geographic analysis analogous to the GWR analysis performed on LST and NDVI, the values of heat-risk variables among SPAs with lowest and highest cooling potentials (Table 4) suggest that the distribution of heat-vulnerable subpopulations in cities is also spatially heterogeneous. Identification of these subpopulations requires the inclusion of spatial terms in order to understand the socio-spatial complexity of temperature, land covers, and populations at risk. As Uejio et al. (2011, p. 498) have said, "failing to account for spatial autocorrelation can provide misleading statistical results."

a. *Limitations of our study*

The methods and data sources used in this paper, consisting of remotely sensed measurements of the surface UHI, have some limitations. First, besides vegetation coverage estimates like those used in this paper, other factors, such as vegetation composition and configuration, affect the temperature reduction potential of vegetated canopies. Assessing the influence of composition and configuration of vegetation (as well as of other elements of the built environment) on regulating temperatures requires higher spatial and spectral resolution than that of the Landsat imagery used in our study (Connors et al. 2013). Our approach, based on Landsat imagery and geostatistical modeling, did not consider this variable. Second, our remote-sensing approach requires calibration of measurements to account for intervening atmosphere and surface radiative properties, both factors that influence emission and radiation detected by the Landsat sensor. We addressed this by conducting atmospheric correction on the ensemble of Landsat images. Third, remotely sensed data provide an indirect measurement that does not capture the full, three-dimensional complexity of urban surfaces. Landsat data used in this paper do not include surface roughness—an indicator of variability in vertical and horizontal textures in the urban environment, implying that our Cleveland UHI description is limited to horizontal surfaces of land covers. Notwithstanding the limitations of remotely sensed data, our study makes use of easily accessible data and employs a reproducible method for quantifying the surface UHI with a good degree of both spatial and temporal (seasonal) detail.

b. *Potential for mitigation and adaptation*

Our research has relevance for climate change mitigation and adaptation in Cleveland. The potential surface temperature reductions under the vegetated possible tree canopy increase estimates in the Cuyahoga County "Urban Tree Canopy Assessment" can be used to identify statistical planning areas to target for establishing green zoning and land-use codes or green infrastructure—two mitigation and adaptation interventions identified by the "Cleveland Climate Action Plan" (Sustainable Cleveland 2013) to reduce greenhouse gas emissions and increase resilience against the impacts of climate change. Specifically, our work can inform the development and implementation of Cleveland's update to its urban tree plan (Action 27 in the "Climate Action Plan") by addressing tree canopy deficits and temperature reduction potentials in specific statistical planning areas in the city. Deployment of an urban tree plan informed by UHI-mitigation considerations can lower temperatures, help reduce exposure to outdoor extreme heat, improve public health (another goal of the action plan), contribute to mitigate greenhouse gases emissions by reducing demand for power generation, and increase atmospheric carbon dioxide absorption and storage.

Establishing temperature reduction goals can be useful to increase the potential for adaptation by estimating reduction of disparities among vulnerable populations, for example, in outcomes of heat-related mortality and morbidity. Temperature reduction goals can be evaluated by estimating temperature thresholds beyond which observed heat-related mortality or morbidity increase markedly. McMichael et al. (2008) have made some progress in this direction by reporting the temperature ranges in which heat-related mortality increased in cities in low- and middle-income countries. These thresholds were found to be higher for cities with hotter summers, signaling that populations in those cities display higher adaptation capacity to adverse heat health outcomes. Kovats et al.

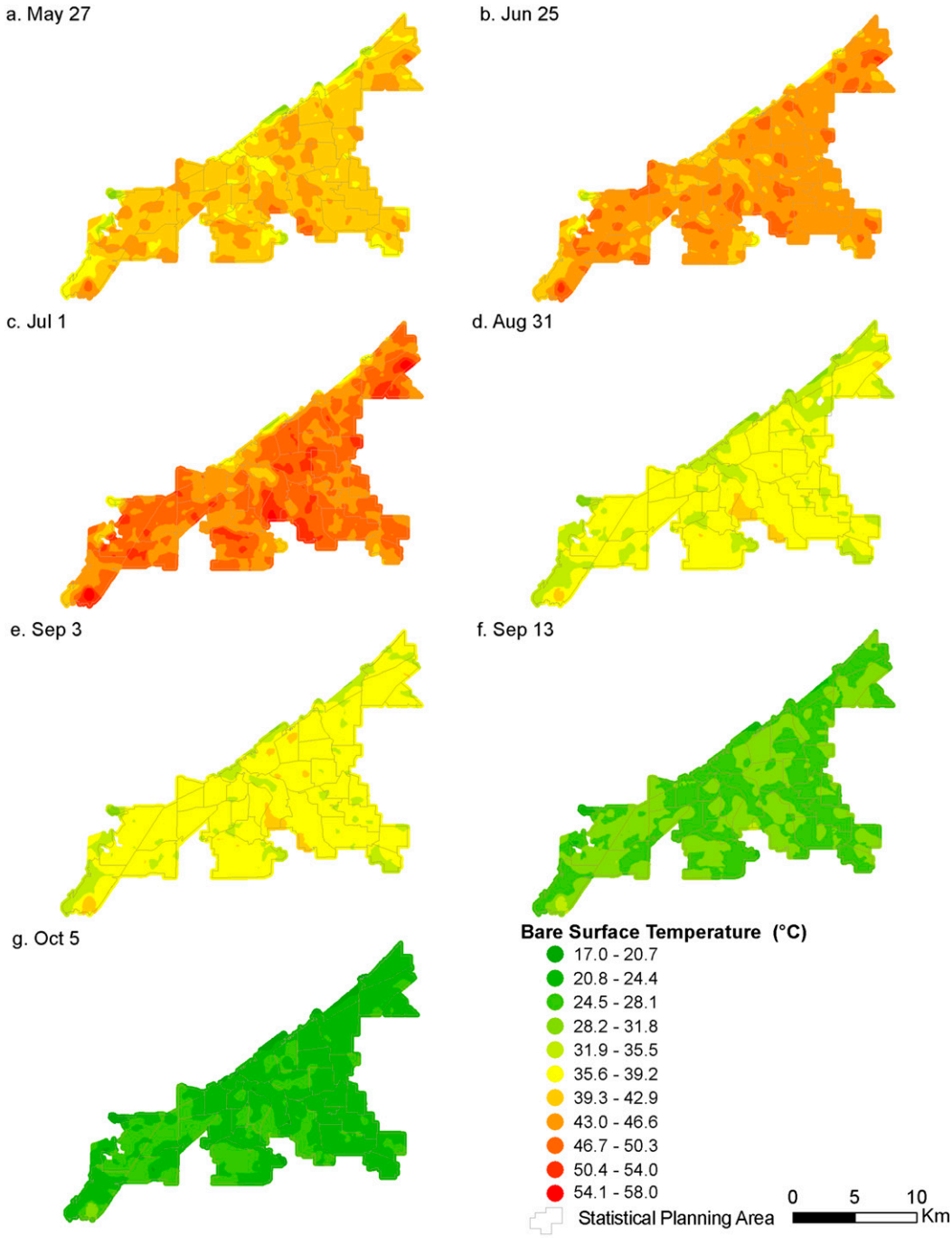

FIG. 4. BST estimates (β_0) from GWR runs for May–October. Estimates are significant at the 95% confidence interval. Statistical planning areas are overlaid for reference.

(2004) evaluated admission cause–specific, and admission cause– and age group–specific temperature thresholds for hospital admissions, but the utility of their thresholds for implementing adaptation or intervention measures is unclear, given that many of their estimates of change in hospitalizations per degree Celsius increase are not statistically significant. These examples point to the difficulties of establishing temperature thresholds useful for public health interventions; as McGeehin and Mirabelli (2001) have argued about U.S. cities, heat tolerance varies regionally according to heat preparedness among the population, and, perhaps more importantly, local mean

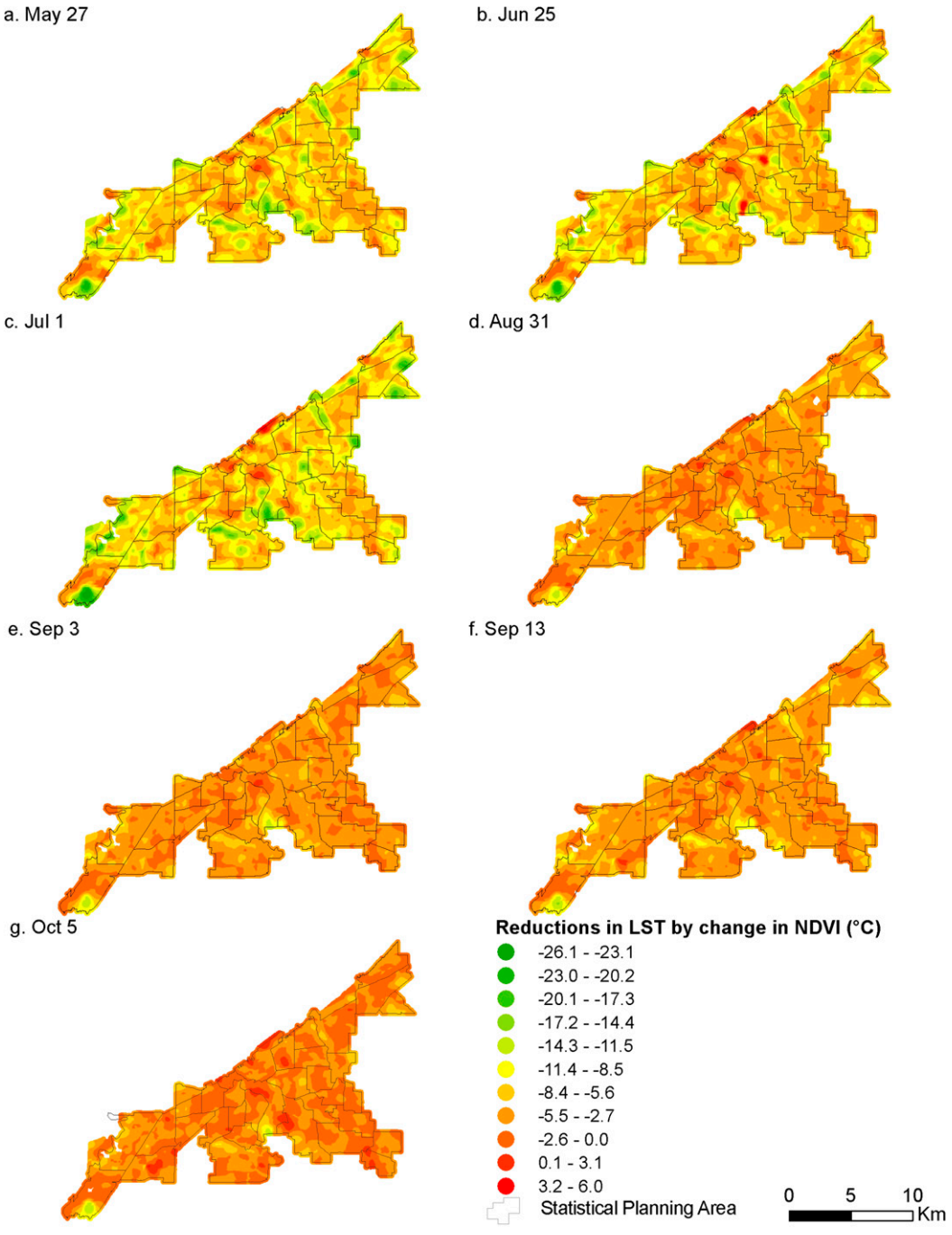

FIG. 5. NDVI local regression coefficients (β_1) from GWR runs for May–October. Estimates are significant at the 95% confidence interval. Statistical planning areas are overlaid for reference.

temperatures and the frequency of temperature extremes. Besides these issues, estimating temperature thresholds useful for planning heat health adaptations requires developing heat-related mortality and/or morbidity rates across vulnerable subpopulations, and such data, typically obtained from county coroner death certificates or emergency department/inpatient hospitalization records, were not available for this study, and this remains an area for future research.

c. *Addressing tree canopy inequity through the urban planning process*

The potential for cooling estimated in our research is directly related to VPTC percentages. Consequently,

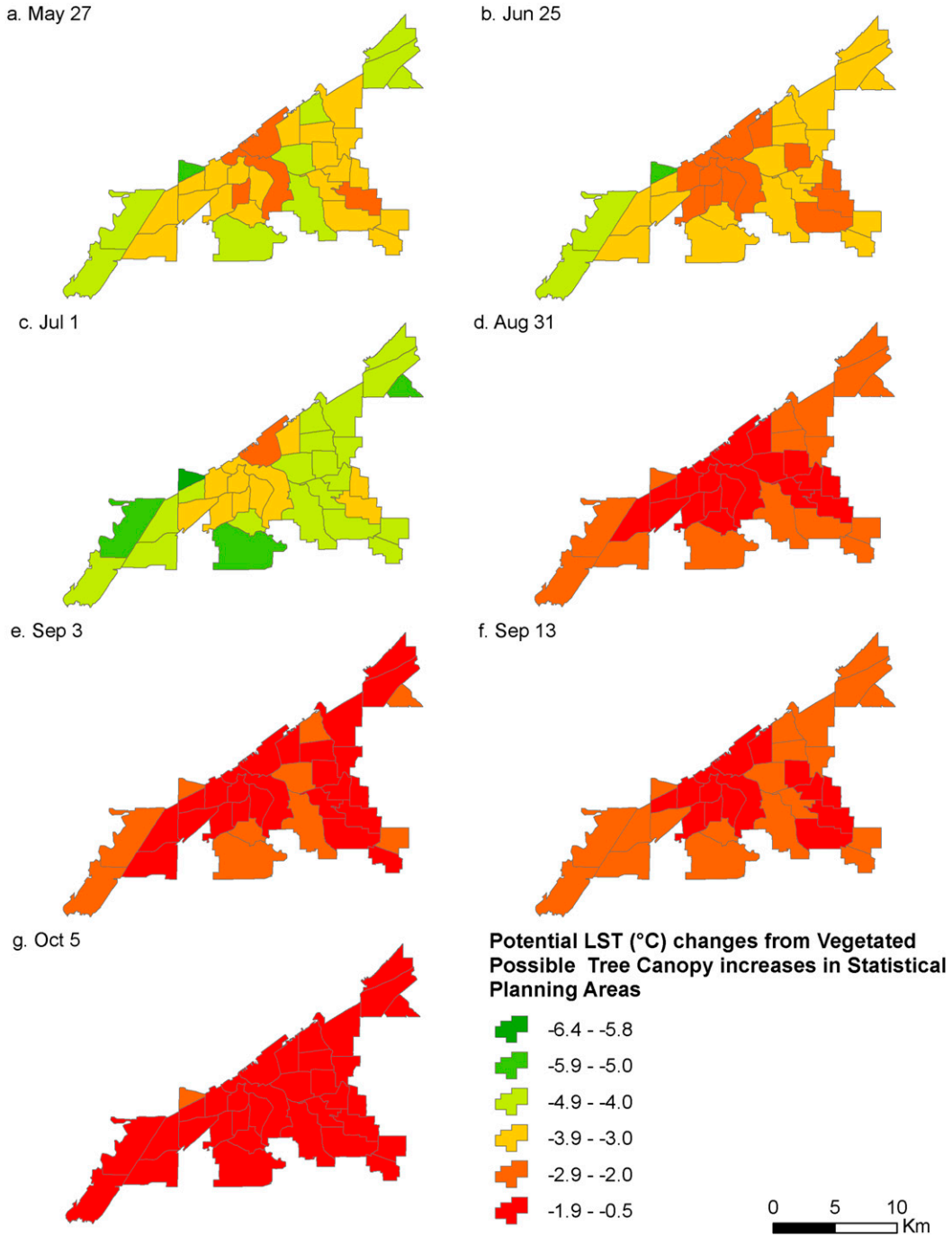

FIG. 6. Potential LST (°C) reductions from vegetated possible tree canopy increases in statistical planning areas in Cleveland, Ohio.

the lowest LST reduction potentials are found in neighborhoods with low VPTC, and a vulnerable population (Hispanics) is concentrated in neighborhoods with some of the lowest VPTC values. Addressing tree canopy inequity in the urban planning process by increasing the vegetation-based cooling potential in neighborhoods with low VPTC and high percentages of vulnerable populations could be achieved through land-use/land-cover alterations that increase VPTC (e.g., reverting impervious surfaces to soil, grass, or ultimately tree canopy). However, this appears unlikely given contestations in the planning process around resources like water and tax dollars to

TABLE 3. Mean potential LST (°C) reductions from vegetated possible tree canopy increases in statistical planning areas in Cleveland, Ohio.

SPA	27 May (°C)	25 Jun (°C)	1 Jul (°C)	31 Aug (°C)	3 Sep (°C)	13 Sep (°C)	5 Oct (°C)
Bellaire-Puritas	3.57	3.57	−0.65	2.08	1.98	2.13	1.26
Broadway-Slavic Village	4.12	3.82	4.76	2.10	2.08	2.27	1.57
Brooklyn Centre	3.74	3.75	4.54	1.98	2.02	2.10	1.54
Buckeye-Shaker Square	3.08	2.57	3.24	1.41	1.45	1.88	1.24
Buckeye-Woodhill	3.36	3.03	4.05	1.78	1.75	1.86	1.22
Central	4.07	3.28	4.90	1.92	2.29	2.15	1.64
Clark-Fulton	2.79	2.67	3.16	1.39	1.38	1.49	1.10
Collinwood-Nottingham	4.26	3.87	4.63	2.57	1.79	2.29	1.30
Cudell	3.46	3.43	4.06	1.77	1.78	1.90	1.60
Cuyahoga Valley	2.90	2.08	3.24	1.53	1.56	1.54	1.18
Detroit Shoreway	3.27	2.88	3.57	1.41	1.56	1.59	1.13
Downtown	2.44	2.21	2.15	1.17	1.37	1.17	0.88
Edgewater	5.35	5.05	6.37	2.48	2.48	2.78	2.44
Euclid-Green	4.70	3.96	5.64	2.58	2.22	2.78	1.97
Fairfax	3.35	2.76	4.46	1.87	1.88	1.75	1.45
Glenville	3.93	3.47	4.35	2.17	1.76	2.26	1.46
Goodrich-Kirtland Park	3.29	2.65	3.12	1.58	1.60	1.44	1.11
Hopkins	4.05	4.02	4.78	2.08	2.12	2.40	1.81
Hough	3.83	3.35	4.37	2.16	1.76	2.18	1.55
Jefferson	3.60	3.19	4.02	1.84	1.87	2.18	1.46
Kamm's	4.50	4.25	5.33	2.26	2.24	2.63	2.00
Kinsman	3.89	3.76	4.88	1.94	1.98	2.17	1.56
Lee-Harvard	3.88	3.98	4.81	2.37	2.15	2.33	1.72
Lee-Seville	3.78	3.74	4.34	2.27	1.87	2.20	1.04
Mount Pleasant	2.82	2.59	3.22	1.48	1.48	1.57	1.27
North Shore Collinwood	4.14	3.70	4.75	2.31	1.79	2.21	1.5
Ohio City	3.11	2.83	3.43	1.62	1.60	1.81	1.38
Old Brooklyn	4.26	3.91	5.2	2.26	2.27	2.41	1.81
Tremont	3.13	2.83	3.79	1.53	1.66	1.64	1.16
Union-Miles	3.31	2.94	4.10	2.01	1.82	1.99	1.38
University	3.81	3.44	4.91	2.14	1.94	2.09	1.83
West Boulevard	3.42	3.32	3.95	1.75	1.76	2.05	1.53
St. Clair-Superior	4.19	3.74	4.36	2.27	2.04	2.26	1.63
Stockyards	3.08	2.86	3.66	1.44	1.62	1.70	1.10

develop and maintain urban green spaces (Declet-Barreto et al. 2013) and siting of urban revegetation projects (Heynen 2003). Increasing tree canopy in areas of highest deficits may be further constrained by tree maintenance and upkeep considerations in urban revegetation projects, which typically target owner-occupied residential properties and exclude renters, presenting an impediment to lower-income populations

TABLE 4. Socioeconomic status and heat-risk variables for statistical planning areas with lowest and highest LST reduction potentials in Cleveland. The highest LST potentials were in Edgewater, Euclid-Green, and Kamm's, while the lowest potentials were in Buckeye-Shaker Square, Clark-Fulton, Downtown, and Goodrich-Kirtland Park.

SPA	Percent black	Percent white	Percent Hispanic	Percent in poverty	Percent no HS diploma	Percent no AC	Percent elderly	Percent living alone	Percent elderly and alone
Edgewater	20.9	65.1	10.4	31.3	22.1	85.5	14.5	58.5	14.2
Euclid-Green	91.8	6.0	1.0	26.5	19.4	91.8	12.8	40.4	8.9
Kamm's	9.5	79.2	7.5	10.4	11.2	70.6	15.9	38.3	13.0
Buckeye-Shaker Square	80.4	13.4	1.6	25.4	17.0	94.4	15.5	50.9	14.5
Clark-Fulton	17.5	32.2	48.3	39.7	38.2	96.4	8.4	29.0	6.4
Downtown	43.5	43.0	3.6	17.0	19.3	34.1	2.5	70.3	3.9
Goodrich-Kirtland Park	25.3	35.7	10.4	15.0	23.5	96.9	2.9	66.8	4.3

from enjoying the benefits of urban greening (Perkins et al. 2004).

Our research contributes to the evaluation of a technical solution—the application of vegetation—to highly heterogeneous summertime heat, a socio-spatial expression of historical and persistent socio-environmental inequities. Notwithstanding the demonstrated cooling potential of vegetation in this paper, tree planting policies based exclusively on such criteria, as measured by vegetation increase potentials, could lead to increasing inequities and unjust distributions of urban tree canopies by prioritizing canopy density increases in areas with existing urban forest islands [i.e., in or near higher-income neighborhoods (Heynen 2006)]. To avoid inadvertently creating or exacerbating inequities, we must engage "critically in planning efforts to produce more equitable urban environments for everyone" (Heynen 2006, p. 20). Canopied vegetation increases should be seen as one component of a multifaceted approach to redressing socio-environmental inequities through an urban planning process that mitigates not just observable effects (e.g., higher summertime temperatures in low-socioeconomic-status neighborhoods), but also the factors in the regional political economy that contribute to the production of such inequities (e.g., income inequality, uneven residential ownership rates, and urban greening focus on private property). In this regard, a planning process engaging multiple scales of governance (municipal, regional, state, and federal) could, for example, facilitate increases in homeownership rates among low-income communities. Higher homeownership rates could help extend to low-income communities the range of modifications homeowners can make to reduce both indoor and outdoor temperatures and energy consumption (especially tree planting), thereby decreasing economic burdens—and, potentially, health burdens—associated with extreme heat. Addressing socioeconomic disparities in income and housing tenure can augment the availability and effectiveness of vegetation-based cooling in cities like Cleveland: research in other Midwestern cities has shown that urban tree canopy declines over time are related to household income [Indianapolis (Heynen 2006)], and lower rates of residential urban tree cover are associated with percentages of minorities and residential renters [Milwaukee (Heynen et al. 2006)].

Addressing the needs of vulnerable communities in the urban planning process is essential because the vulnerable are "often unable to produce local and healthy urban ecologies for themselves" (e.g., via disposable income to pay for tree planting and maintenance) (Heynen 2006, p. 5), relying on public planting of street trees and the creation of public green spaces. In this paper, we have shown that vegetation can provide UHI-mitigating ecosystem services and that cooling potentials vary considerably both within the built environment, according to vegetation planting potentials, and socio-spatially among vulnerable populations. Our study identifies areas of Cleveland that can be targeted for UHI-mitigation action under the city's Climate Adaptation Plan to reduce heat exposure among the most vulnerable populations and urges policymakers to address broader equity concerns by formulating policies that mitigate, together with vegetation-based UHI interventions, the production of heat-related socio-environmental inequities.

Acknowledgments. This research was made possible by a grant from the Natural Resources Defense Council's Science Center. The authors declare that there are no conflicts of interest.

REFERENCES

Arnfield, A., 2003: Two decades of urban climate research: A review of turbulence, exchanges of energy and water, and the urban heat island. *Int. J. Climatol.*, **23**, 1–26, doi:10.1002/joc.859.

Balling, R. C., and S. W. Brazel, 1987: The impact of rapid urbanization on pan evaporation in Phoenix, Arizona. *J. Climatol.*, **7**, 593–597, doi:10.1002/joc.3370070607.

Bobb, J. F., R. D. Peng, M. L. Bell, and F. Dominici, 2014: Heat-related mortality and adaptation to heat in the United States. *Environ. Health Perspect.*, **122**, 811–816, doi:10.1289/ehp.1307392.

Boumans, R. J., D. L. Phillips, W. Victery, and T. D. Fontaine, 2014: Developing a model for effects of climate change on human health and health–environment interactions: Heat stress in Austin, Texas. *Urban Climate*, **8**, 78–99, doi:10.1016/j.uclim.2014.03.001.

Buscail, C., E. Upegui, and J.-F. Viel, 2012: Mapping heatwave health risk at the community level for public health action. *Int. J. Health Geogr.*, **11**, 38, doi:10.1186/1476-072X-11-38.

Buyantuyev, A., and J. Wu, 2010: Urban heat islands and landscape heterogeneity: Linking spatiotemporal variations in surface temperatures to land-cover and socioeconomic patterns. *Landscape Ecol.*, **25**, 17–33, doi:10.1007/s10980-009-9402-4.

Chow, W. T. L., R. L. Pope, C. A. Martin, and A. J. Brazel, 2011: Observing and modeling the nocturnal park cool island of an arid city: Horizontal and vertical impacts. *Theor. Appl. Climatol.*, **103**, 197–211, doi:10.1007/s00704-010-0293-8.

Cleveland City Planning Commission, 2014a: 2014 Neighborhood fact sheets. Accessed 6 July 2015. [Available online at http://planning.city.cleveland.oh.us/2010census/factsheets.php.]

——, 2014b: 8 ideas for vacant land re-use in Cleveland. Accessed 10 October 2014. [Available online at http://planning.city.cleveland.oh.us/ftp/8IdeasForVacantLandReuseCleveland.pdf.]

Connors, J. P., C. S. Galletti, and W. T. Chow, 2013: Landscape configuration and urban heat island effects: Assessing the relationship between landscape characteristics and land surface temperature in Phoenix, Arizona. *Landscape Ecol.*, **28**, 271–283, doi:10.1007/s10980-012-9833-1.

Cuyahoga County Geographical Information Systems, 2016: Cities shapefile. Accessed 27 September 2016. [Available online at http://gis.cuyahogacounty.us/en-US/GIS-Data.aspx.]

Cuyahoga County Planning Commission, 2013a: Cuyahoga County GIS parcels dataset. Accessed 6 July 2015. [Available online at ftp.gis.cuyahogacounty.us.]

——, 2013b: Cuyahoga County urban tree canopy assessment. Accessed 6 July 2015. [Available online at http://planning.co.cuyahoga.oh.us/canopy/downloads.html.]

Declet-Barreto, J., A. J. Brazel, C. A. Martin, W. T. Chow, and S. L. Harlan, 2013: Creating the park cool island in an inner-city neighborhood: Heat mitigation strategy for Phoenix, AZ. *Urban Ecosyst.*, **16**, 617–635, doi:10.1007/s11252-012-0278-8.

Filleul, L., and Coauthors, 2006: The relation between temperature, ozone, and mortality in nine French cities during the heat wave of 2003. *Environ. Health Perspect.*, **114**, 1344–1347, doi:10.1289/ehp.8328.

Foody, G., 2003: Geographical weighting as a further refinement to regression modelling: An example focused on the NDVI–rainfall relationship. *Remote Sens. Environ.*, **88**, 283–293, doi:10.1016/j.rse.2003.08.004.

Fotheringham, A. S., C. Brunsdon, and M. Charlton, 2003: *Geographically Weighted Regression: The Analysis of Spatially Varying Relationships.* John Wiley & Sons, 284 pp.

Frey, W. H., and D. Myers, 2005: Racial segregation in U.S. metropolitan areas and cities, 1990–2000: Patterns, trends, and explanations. Population Studies Center Research Rep. 05-573, 66 pp. [Available online at http://www.frey-demographer.org/reports/R-2005-2_RacialSegragationTrends.pdf.]

Gallo, K., A. McNab, T. Karl, J. Brown, J. Hood, and J. Tarpley, 1993: The use of a vegetation index for assessment of the urban heat island effect. *Remote Sens.*, **14**, 2223–2230, doi:10.1080/01431169308954031.

Galster, G. C., 1990: White flight from racially integrated neighbourhoods in the 1970s: The Cleveland experience. *Urban Stud.*, **27**, 385–399, doi:10.1080/00420989020080341.

Gasparrini, A., and Coauthors, 2015: Temporal variation in heat–mortality associations: A multicountry study. *Environ. Health Perspect.*, **123**, 1200–1207, doi:10.1289/ehp.1409070.

Harlan, S. L., A. J. Brazel, L. Prashad, W. L. Stefanov, and L. Larsen, 2006: Neighborhood microclimates and vulnerability to heat stress. *Soc. Sci. Med.*, **63**, 2847–2863, doi:10.1016/j.socscimed.2006.07.030.

——, J. H. Declet-Barreto, W. L. Stefanov, and D. B. Petitti, 2013: Neighborhood effects on heat deaths: Social and environmental predictors of vulnerability in Maricopa County, Arizona. *Environ. Health Perspect.*, **121**, 197–204, doi:10.1289/ehp.1104625.

Hattis, D., Y. Ogneva-Himmelberger, and S. Ratick, 2012: The spatial variability of heat-related mortality in Massachusetts. *Appl. Geogr.*, **33**, 45–52, doi:10.1016/j.apgeog.2011.07.008.

Heisler, G. M., and A. J. Brazel, 2010: The urban physical environment: Temperature and urban heat islands. *Urban Ecosystem Ecology, Agron. Monogr.*, No. 55, American Society of Agronomy, 29–56.

Hewitt, V., E. Mackres, and K. Shickman, 2014: Cool policies for cool cities: Best practices for mitigating urban heat islands in North American cities. American Council for an Energy-Efficient Economy Research Rep. U1405, 15 pp. [Available online at http://www.aceee.org/research-report/u1405.]

Heynen, N., 2003: The scalar production of injustice within the urban forest. *Antipode*, **35**, 980–998, doi:10.1111/j.1467-8330.2003.00367.x.

——, 2006: Green urban political ecologies: Toward a better understanding of inner-city environmental change. *Environ. Plann.*, **38A**, 499–516, doi:10.1068/a37365.

——, H. A. Perkins, and P. Roy, 2006: The political ecology of uneven urban green space: The impact of political economy on race and ethnicity in producing environmental inequality in Milwaukee. *Urban Aff. Rev.*, **42**, 3–25, doi:10.1177/1078087406290729.

Hondula, D. M., R. E. Davis, M. J. Leisten, M. V. Saha, L. M. Veazey, and C. R. Wegner, 2012: Fine-scale spatial variability of heat-related mortality in Philadelphia County, USA, from 1983–2008: A case-series analysis. *Environ. Health*, **11**, 16, doi:10.1186/1476-069X-11-16.

Imhoff, M. L., P. Zhang, R. E. Wolfe, and L. Bounoua, 2010: Remote sensing of the urban heat island effect across biomes in the continental USA. *Remote Sens. Environ.*, **114**, 504–513, doi:10.1016/j.rse.2009.10.008.

Ivajnšič, D., M. Kaligarič, and I. Žiberna, 2014: Geographically weighted regression of the urban heat island of a small city. *Appl. Geogr.*, **53**, 341–353, doi:10.1016/j.apgeog.2014.07.001.

Jenerette, G. D., S. L. Harlan, A. Brazel, N. Jones, L. Larsen, and W. L. Stefanov, 2007: Regional relationships between surface temperature, vegetation, and human settlement in a rapidly urbanizing ecosystem. *Landscape Ecol.*, **22**, 353–365, doi:10.1007/s10980-006-9032-z.

——, ——, W. L. Stefanov, and C. A. Martin, 2011: Ecosystem services and urban heat riskscape moderation: Water, green spaces, and social inequality in Phoenix, USA. *Ecol. Appl.*, **21**, 2637–2651, doi:10.1890/10-1493.1.

Jesdale, B. M., R. Morello-Frosch, and L. Cushing, 2013: The racial/ethnic distribution of heat risk–related land cover in relation to residential segregation. *Environ. Health Perspect.*, **121**, 811–817, doi:10.1289/ehp.1205919.

Jin, S., L. Yang, P. Danielson, C. Homer, J. Fry, and G. Xian, 2013: A comprehensive change detection method for updating the National Land Cover Database to circa 2011. *Remote Sens. Environ.*, **132**, 159–175, doi:10.1016/j.rse.2013.01.012.

Johnson, D. P., and J. S. Wilson, 2009: The socio-spatial dynamics of extreme urban heat events: The case of heat-related deaths in Philadelphia. *Appl. Geogr.*, **29**, 419–434, doi:10.1016/j.apgeog.2008.11.004.

——, ——, and G. C. Luber, 2009: Socioeconomic indicators of heat-related health risk supplemented with remotely sensed data. *Int. J. Health Geogr.*, **8**, 57, doi:10.1186/1476-072X-8-57.

Kaiser, R., A. Le Tertre, J. Schwartz, C. A. Gotway, W. R. Daley, and C. H. Rubin, 2007: The effect of the 1995 heat wave in Chicago on all-cause and cause-specific mortality. *Amer. J. Public Health*, **97** (Suppl. 1), S158–S162, doi:10.2105/AJPH.2006.100081.

Kottek, M., J. Grieser, C. Beck, B. Rudolf, and F. Rubel, 2006: World map of the Köppen–Geiger climate classification updated. *Meteor. Z.*, **15**, 259–263, doi:10.1127/0941-2948/2006/0130.

Kovats, R. S., S. Hajat, and P. Wilkinson, 2004: Contrasting patterns of mortality and hospital admissions during hot weather and heat waves in greater London, UK. *Occup. Environ. Med.*, **61**, 893–898, doi:10.1136/oem.2003.012047.

Li, D., and E. Bou-Zeid, 2013: Synergistic interactions between urban heat islands and heat waves: The impact in cities is larger than the sum of its parts. *J. Appl. Meteor. Climatol.*, **52**, 2051–2064, doi:10.1175/JAMC-D-13-02.1.

Li, S., Z. Zhao, X. Miaomiao, and Y. Wang, 2010: Investigating spatial non-stationary and scale-dependent relationships between urban surface temperature and environmental factors using geographically weighted regression. *Environ. Modell. Software*, **25**, 1789–1800, doi:10.1016/j.envsoft.2010.06.011.

Ma, W., Y.-H. Chen, and J. Zhou, 2008: Quantitative analysis of land surface temperature-vegetation indexes relationship based on remote sensing. *Proc. 21st ISPRS Congress*, *Youth Forum*, Beijing, China, International Society for Photogrammetry and Remote Sensing, 261–264. [Available online at http://www.isprs.org/proceedings/XXXVII/congress/6b_pdf/43.pdf.]

Maselli, F., 2002: Improved estimation of environmental parameters through locally calibrated multivariate regression analyses. *Photogramm. Eng. Remote Sens.*, **68**, 1163–1172.

McGeehin, M. A., and M. Mirabelli, 2001: The potential impacts of climate variability and change on temperature-related morbidity and mortality in the United States. *Environ. Health Perspect.*, **109** (Suppl. 2), 185, doi:10.2307/3435008.

McMichael, A. J., and Coauthors, 2008: International study of temperature, heat and urban mortality: The 'ISOTHERM' project. *Int. J. Epidemiol.*, **37**, 1121–1131, doi:10.1093/ije/dyn086.

Mennis, J., 2006: Mapping the results of geographically weighted regression. *Cartographic J.*, **43**, 171–179, doi:10.1179/000870406X114658.

Minnesota Population Center, 2016a: American community survey: 5-year data [2006–2010, block groups and larger areas]. National Historical Geographic Information System, version 2.0. Subset used: Tables B15002: Sex by educational attainment for the population 25 years and over; and C17002: Ratio of income to poverty level in the past 12 months. Accessed 22 September 2016. [Available online at http://www.nhgis.org/.]

——, 2016b: 2010 Census: SF1a—P & H Tables [Block groups and larger areas]. National Historical Geographic Information System, version 2.0. Subset used: Tables P7: Hispanic or Latino origin by race (total races tallied); P12: Sex by age; and P25: Households by presence of people 65 years and over, household size, and household type. Accessed 22 September 2016. [Available online at http://www.nhgis.org/.]

Mohamed, M., 2013: Summer land surface temperature: Small-local variation in intro-urban environment in El Paso, TX. Ph.D. dissertation, The University of Texas at El Paso, 145 pp.

NCEI, 2015: Daily summaries for air temperature at Cleveland Burke Lake Airport, OH. NCEI, accessed 22 September 2016. [Available online at http://www.ncdc.noaa.gov/cdo-web/.]

Oke, T. R., 1997: The changing climatic environments: Urban climates and global environmental change. *Applied Climatology Principals and Practice*, R. D. Thompson and A. Perry, Eds., Routledge, 273–287.

——, 2006: Towards better scientific communication in urban climate. *Theor. Appl. Climatol.*, **84**, 179–190, doi:10.1007/s00704-005-0153-0.

Onishi, A., X. Cao, T. Ito, F. Shi, and H. Imura, 2010: Evaluating the potential for urban heat-island mitigation by greening parking lots. *Urban For. Urban Greening*, **9**, 323–332, doi:10.1016/j.ufug.2010.06.002.

Pattenden, S., and Coauthors, 2010: Ozone, heat and mortality: Acute effects in 15 British conurbations. *Occup. Environ. Med.*, **67**, 699–707, doi:10.1136/oem.2009.051714.

Perkins, H., N. Heynen, and J. Wilson, 2004: Inequitable access to urban reforestation: The impact of urban political economy on housing tenure and urban forests. *Cities*, **21**, 291–299, doi:10.1016/j.cities.2004.04.002.

Reid, C. E., and Coauthors, 2012: Evaluation of a heat vulnerability index on abnormally hot days: An environmental public health tracking study. *Environ. Health Perspect.*, **120**, 715–720, doi:10.1289/ehp.1103766.

Ruddell, D. M., S. L. Harlan, S. Grossman-Clarke, and A. Buyantuyev, 2010: Risk and exposure to extreme heat in microclimates of Phoenix, AZ. *Geospatial Techniques in Urban Hazard and Disaster Analysis*, P. S. Showalter and Y. Lu, Eds., Geotechnologies and the Environment, Vol. 2, Springer, 179–202, doi:10.1007/978-90-481-2238-7_9.

Salamanca, F., M. Georgescu, A. Mahalov, M. Moustaoui, and M. Wang, 2014: Anthropogenic heating of the urban environment due to air conditioning. *J. Geophys. Res. Atmos.*, **119**, 5949–5965, doi:10.1002/2013JD021225.

Sheridan, S. C., A. J. Kalkstein, and L. S. Kalkstein, 2009: Trends in heat-related mortality in the United States, 1975–2004. *Nat. Hazards*, **50**, 145–160, doi:10.1007/s11069-008-9327-2.

Stone, B., J. Vargo, P. Liu, D. Habeeb, A. DeLucia, M. Trail, Y. Hu, and A. Russell, 2014: Avoided heat-related mortality through climate adaptation strategies in three US cities. *PloS One*, **9**, e100852, doi:10.1371/journal.pone.0100852.

Su, Y.-F., G. M. Foody, and K.-S. Cheng, 2012: Spatial nonstationarity in the relationships between land cover and surface temperature in an urban heat island and its impacts on thermally sensitive populations. *Landscape Urban Plann.*, **107**, 172–180, doi:10.1016/j.landurbplan.2012.05.016.

Sun, D., and M. Kafatos, 2007: Note on the NDVI–LST relationship and the use of temperature-related drought indices over North America. *Geophys. Res. Lett.*, **34**, L24406, doi:10.1029/2007GL031485.

Sustainable Cleveland, 2013: Cleveland Climate Action Plan: Building thriving and healthy neighborhoods. [Available online at https://d3n8a8pro7vhmx.cloudfront.net/sustainablecleveland/pages/149/attachments/original/1461798511/Cleveland_Climate_Action_Plan.pdf?1461798511.]

Szymanowski, M., and M. Kryza, 2011: Application of geographically weighted regression for modelling the spatial structure of urban heat island in the city of Wroclaw (SW Poland). *Procedia Environ. Sci.*, **3**, 87–92, doi:10.1016/j.proenv.2011.02.016.

Tucker, C. J., 1979: Red and photographic infrared linear combinations for monitoring vegetation. *Remote Sens. Environ.*, **8**, 127–150, doi:10.1016/0034-4257(79)90013-0.

Uejio, C. K., O. V. Willhelmi, J. S. Golden, D. M. Mills, S. P. Gulino, and J. P. Samenow, 2011: Intra-urban societal vulnerability to extreme heat: The role of heat exposure and the built environment, socioeconomics, and neighborhood stability. *Health Place*, **17**, 498–507, doi:10.1016/j.healthplace.2010.12.005.

U.S. Census Bureau, 2014: State and county QuickFacts: Cleveland (city), Ohio. Accessed 18 October 2016. [Available online at http://quickfacts.census.gov/qfd/states/39/3916000.html.]

USGS, 2016: USGS global visualization viewer. Accessed 5 May 2016. [Available online at http://glovis.usgs.gov.]

Voogt, J. A., and T. Oke, 1998: Effects of urban surface geometry on remotely-sensed surface temperature. *Int. J. Remote Sens.*, **19**, 895–920, doi:10.1080/014311698215784.

——, and T. R. Oke, 2003: Thermal remote sensing of urban climates. *Remote Sens. Environ.*, **86**, 370–384, doi:10.1016/S0034-4257(03)00079-8.

White-Newsome, J. L., S. J. Brines, D. G. Brown, J. T. Dvonch, C. J. Gronlund, K. Zhang, E. M. Oswald, and M. S. O'Neill, 2013: Validating satellite-derived land surface temperature with in situ measurements: A public health perspective. *Environ. Health Perspect.*, **121**, 925–931, doi:10.1289/ehp.1206176.

——, B. Ekwurzel, M. Baer-Schultz, K. L. Ebi, M. S. O'Neill, and G. B. Anderson, 2014a: Survey of county-level heat preparedness and response to the 2011 summer heat in 30 U.S.

states. *Environ. Health Perspect.*, **122**, 573–574, doi:10.1289/ehp.1306693.

——, and Coauthors, 2014b: Strategies to reduce the harmful effects of extreme heat events: A four-city study. *Int. J. Environ. Res. Public Health*, **11**, 1960–1988, doi:10.3390/ijerph110201960.

Yip, F., and Coauthors, 2008: The impact of excess heat events in Maricopa County, Arizona: 2000–2005. *Int. J. Biometeor.*, **52**, 765–772, doi:10.1007/s00484-008-0169-0.

Yuan, F., and S. S. Roy, 2007: Analysis of the relationship between NDVI and climate variables in Minnesota using geographically weighted regression and spatial interpolation. *Proc. ASPRS 2007 Annual Conf.*, Tampa, FL, American Society for Photogrammetry and Remote Sensing, 784–789.

Yue, W., J. Xu, W. Tan, and L. Xu, 2007: The relationship between land surface temperature and NDVI with remote sensing: Application to Shanghai Landsat 7 ETM+ data. *Int. J. Remote Sens.*, **28**, 3205–3226, doi:10.1080/01431160500306906.